

pubs.acs.org/crystal Article

Rutin Cocrystals with Improved Solubility, Bioavailability, and Bioactivities

Bingrui Zhang, Lei Tang, Fanyu Tian, Qiaoce Ding, Ziyi Hu, Jian-Rong Wang,* and Xuefeng Mei*



Cite This: https://doi.org/10.1021/acs.cgd.4c00430



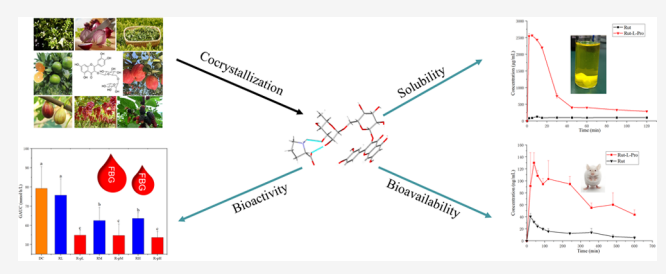
ACCESS I

III Metrics & More

Article Recommendations

s Supporting Information

ABSTRACT: Rutin is a natural compound that is widely distributed in various plants. Increasing lines of evidence have proved that rutin has a beneficial effect on cardiovascular health, oxidative stress, and blood glucose control. However, the application of rutin is limited due to its poor solubility and low oral bioavailability. To improve the bioavailability of rutin, two cocrystals of rutin with L-proline and D-proline were prepared successfully, and multiple characterization methods were utilized to study the physicochemical properties of rutin and its cocrystals. The powder dissolution *in vitro* and the pharmacokinetic behavior



in vivo were also evaluated. The results indicated that Rut-L-Pro exhibited a significantly improved solubility, and the oral bioavailability also had great improvement; the AUC_{0-10h} of Rut-L-Pro was 5.6-fold that of rutin, and C_{max} was 3.8 times. As a result of the improvement of rutin bioavailability, Rut-L-Pro performed better blood glucose control and cardioprotective activities.

■ INTRODUCTION

Rutin (vitamin P, Scheme 1) is a natural bioflavonoid that exists in a wide variety of plants such as buckwheat, grapes,

Scheme 1. Chemical Structure of Rutin

onions, *Sophora japonica*, *etc.* Buckwheat is one of the most important sources of rutin. Due to the chemical structure with polyphenolic hydroxyl, rutin has a variety of physiological activities such as antioxidant, anti-inflammatory, anticancer, neuroprotective, and antidiabetic. In neuroprotective, are cardioprotective, and antidiabetic.

The antioxidant activity of rutin was evaluated by different assays, and the results indicated that rutin exhibited significant 1,1-diphenyl-2-picryl-hydrazyl (DPPH) radical scavenging activity with 90.4% inhibition. Cardiovascular disease has been a great challenge for human health care, which results in irreversible myocardial injury, and rutin has been proven to exhibit great cardioprotective effects by regulating cardiomyocyte autophagy and apoptosis, decreasing the degree of mitochondrial damage, reducing the hypertrophic signaling,

and improving the antioxidant status.¹⁷ Xianchu et al. proved that pretreatment with rutin alleviated the myocardial injury induced by lipopolysaccharide and decreased the levels of creatine kinase (CK) and lactic dehydrogenase (LDH) in serum. The research also proposed that treatment with rutin attenuated the expression of matrix metalloproterinase-2 and matrix metalloproterinase-9. 18 Another research study reported the protective effect of rutin for diabetic cardiomyopathy (DCM). It was found that administration with rutin can significantly improve myocardial hypertrophy caused by diabetes, decrease the levels of cardiomyopathy biomarkers, and improve the antioxidant status.¹⁹ Moreover, a great number of research studies proposed that rutin has a beneficial effect on blood glucose control, and the mechanisms of the antihyperglycemic effect of rutin include inhibiting α glucosidases and α -amylase, stimulating insulin secretion, and promoting tissue glucose uptake. 20-22 Jadhav et al. evaluated the antidiabetic activity of boswellic acid, ellagic acid, quercetin, and rutin. It could be found that rutin performed the most significant effect on decreasing the glucose tolerance at the same dose, where boswellic acid, ellagic acid, quercetin, and rutin declined 5.45, 6.13, 3.41, and 9.53%, respectively, compared with the control group at a dosage of 100 mg/kg.

Received: March 27, 2024 Revised: June 4, 2024 Accepted: June 4, 2024



Niture et al. studied the antidiabetic activity of rutin at different doses, and the results indicated that oral administration of rutin reduced the level of fast blood glucose (FBG) and decreased the formation of advanced glycation end-product precursors, TNF- α and IL-6. The study also proposed that rutin performed a dose-related blood glucose control effect. Moreover, rutin increased the expression of endogenous antioxidant enzymes (glutathione, superoxide dismutase, and catalase) and improved oxidative stress subsequently. In conclusion, rutin is a natural compound with low toxicity, has been proven to process multiple bioactivities including antidiabetic, neuroprotection, heart protection, and liver protection, and can be used as a beneficial human supplement for improving cardiovascular health, oxidative stress, and blood glucose control.

However, the low solubility in water (about 125 μ g/mL) and low oral bioavailability (4.9% in Sprague-Dawley rats) of rutin limited its application. ^{25,26} Various systems including nanocrystals, ²⁷ solid dispersion, ²⁸ self-double-emulsifying delivery system (SDEDS), ²⁶ and solid lipid nanoparticles²⁹ have been used for improving rutin solubility. Mauludin et al. prepared rutin nanocrystals by lyophilization. Nanocrystalloaded tablets dissolved completely within 30 min, while market tablets dissolved about 60% of rutin. 30,31 The solid dispersions of rutin were obtained by solvent evaporation at a weight ratio of 1:1. Rutin-PVP K30 SD exhibited a higher equilibrium solubility compared with pure rutin. ³² Paczkowska et al. obtained a rutin- β -cyclodextrin complex by cogrinding, and the solubility of rutin and the rutin- β -cyclodextrin complex was studied. The rutin- β -cyclodextrin complex showed higher solubility in different buffers.³³ Wang et al. developed a nonaqueous self-double-emulsifying delivery system (SDEDS) containing rutin, which significantly improved the dissolution rate. The oral bioavailability increased from 4.9 to 8.62%, 1.76 times that of the raw material.²⁶ However, there are few reports about utilizing cocrystallization techniques to improve the solubility of rutin. Only a few studies reported the solvates of rutin, and the crystal structure of rutin peneamethanol was solved successfully. The crystals were orthorhombic, and the space group was C222₁. ³⁴ Generally, two or more different molecules combined in the same lattice at a certain stoichiometric ratio by noncovalent interactions are regarded as cocrystals.³⁵ The reasons are as follows: (1) There is no change in the structure so that there is no influence on drug activity, (2) both non-ionized and weakly ionized molecules can form cocrystals theoretically, and (3) quantity coformers with high safety can be utilized for cocrystallization,³⁶ and cocrystallization has been a common skill to improve the physicochemical properties of various compounds.

Therefore, we aimed to obtain a new solid form of rutin with higher water solubility and better physicochemical properties by cocrystallization. We prepared the cocrystals of rutin with L-proline and D-proline successfully. Rut-L-Pro exhibited the best physicochemical properties and significantly improved solubility compared with parent rutin. The bioavailability of Rut-L-Pro increased sharply, which was consistent with the improvement of solubility. The improvement of bioavailability also resulted in better bioactivities.

MATERIALS AND METHODS

Materials. Rutin trihydrate (purity >96%) was purchased from Beijing Innochem Technology Co., Ltd. Coformers were obtained from Shanghai Aladdin Biochemical Technology Co., Ltd., Shanghai,

China. All of the solvents used in the study were analytic grade and were obtained from Sinopham Chemical Reagent Co., Ltd., Shanghai, China. Moreover, β -glucuronidase and sulfatase were obtained from Sigma-Aldrich (Shanghai) Co., Ltd. The superoxide dismutase (SOD) diagnostic biochemical assay kit was purchased from Nanjing Jiancheng Biotechnology Institute, Nanjing, China. The creatine kinase (CK), creatine kinase-MB (CK-MB), and lactate dehydrogenase (LDH) diagnostic biochemical assay kits were purchased from Beijing Huayu Yikang Biotechnology Co., Ltd. pH 2.0, 4.5, and 6.8 buffers can be prepared as follows.

The pH 2.0 buffer used 0.2 mol/L hydrochloric acid and 0.2 mol/L phosphate to adjust the pH value. The pH 4.5 buffer was composed of citric acid monohydrate and phosphate, while the pH 6.8 buffer utilized sodium dihydrogen phosphate and dibasic sodium phosphate. Streptozotocin was dissolved in the buffer consisting of citric acid and sodium citrate. All reagents were used without further purification in this research.

Preparation of Rutin Cocrystals. The preparation method of cocrystals mainly included the solid-state method and solution-based method. The solid-state method referred to neat grinding and liquid-assisted grinding, while the solution-based method contained slurry conversion, solution crystallization, and solvent evaporation.³⁷ More than 40 coformers were screened, and 2 cocrystals were obtained finally, *i.e.*, Rut-L-Pro and Rut-D-Pro. Both cocrystals of rutin were prepared by slurring.

About 3 g (5 mmol) of rutin and a stoichiometric amount of L-proline were added to 100 mL of ethanol and then stirred at 800 rpm overnight. All operations were performed at room temperature. The cocrystal (rutin/L-proline/3 H_2O , 1:1:3) was synthesized after drying at room temperature, and powder X-ray diffraction (PXRD) confirmed whether there was a new solid form generated.

Rut-D-Pro (rutin/D-proline, 1:2) was prepared by utilizing the same method and was further characterized by PXRD, differential scanning calorimetry (DSC), thermogravimetric analysis (TGA), and infrared (IR). The ratio of rutin and D-proline in Rut-D-Pro was determined to be 1:2 using 1H NMR (600 MHz, CD $_3$ OD), which is illustrated in Figure S1. The signals at 2.09 (dq, 2H) ppm and 2.32–2.23 (m, 2H) ppm belonged to the two hydrogen atoms in the tetrahydropyrrole ring of D-proline. The signal at 1.09 (d, 3H) ppm corresponded to the hydrogen atoms of the methyl group in rutin, and the ratio of rutin and D-proline was confirmed to be 1:2.

Preparation of Single Crystals. We obtained single crystals of Rut-L-Pro by slow evaporation. About 60 mg of Rut-L-Pro was added to 1 mL of the solvent consisting of 50% methanol and 50% ethyl acetate. The sample was filtered, and the supernatant was collected. The solution was placed at room temperature for slow evaporation, and the single crystals were gradually generated after 3–4 days.

Powder X-ray Diffraction (PXRD). A Bruker D8 Advance X-ray diffractometer was used to obtain all of the PXRD patterns. The voltage was set to 40 kV, while the current was set to 40 mA. It scanned 2θ values from 3 to 40° at a speed of 0.1 s/step; all operations were performed at the ambient temperature. The RINT Rapid imaged and integrated the resulting data, and the final peaks were analyzed by Jade 6.0 from Rigaku.

Differential Scanning Calorimetry (DSC). All of the DSC experiments were conducted on a DSC TA Q2000 instrument, and the nitrogen gas flow rate was 50 mL/min. A sealed aluminum pan with 1-5 mg of the sample was heated at a rate of $10~^{\circ}\text{C/min}$.

Thermogravimetric Analysis (TGA). A TGA 55 instrument (TA Instruments, New Castle, DE) was utilized to perform all of the thermogravimetric analysis; the nitrogen gas flow rate was 60 mL/min. A non-hermetic aluminum pan with 5–10 mg of the sample was heated at a rate of 10 °C/min from 25 to 410 °C.

Fourier Transformation Infrared (FT-IR) Spectroscopy. The FT-IR experiments were carried out on a ThermoFisher Nicolet iS50 FT-IR spectrometer, and the samples were scanned in the range of 4000–400 cm⁻¹. The resolution was 4 cm⁻¹.

Dynamic Vapor Absorption (DVS). The water sorption and desorption process of the cocrystals was detected by an Intrinsic DVS (Surface Measurement Systems, Ltd.). The powder sample was

loaded onto the balance. Hygroscopicity behaviors were measured by the relative humidity ranging from 0 to 95% and then decreasing to 0% at 25 $^{\circ}$ C. The humidity step would not proceed unless the mass change was less than 0.02% within 60 min.

Single-Crystal X-ray Diffraction (SCXRD). An APEXII CCD diffractometer (Bruker) with Mo K α (λ = 0.71073 Å) was utilized to conduct the X-ray diffraction collection of Rut-L-Pro under 170 K. The crystal was selected carefully and loaded on the loops, and the program SAINT was used to integrate and scale the intensity data. To remove the influence of the absorption effect, the refinement was performed by SADABS. The crystal structure was analyzed directly by the direct methods on SHELXTL and refined by full-matrix least-squares on SHELXT-2017 software. The CCDC number of Rut-L-Pro was 2323197.

Powder Dissolution Tests. In order to remove the influence of particle size on solubility and powder dissolution, we sifted all of the samples through 100-mesh sieves. The powder dissolution experiments were conducted in the pH 2.0, 4.5, and 6.8 buffers with 1% Tween 80. The research studies were carried out on a mini-bath dissolution instrument with a Julabo-5 heater/circulator. About 50 mg of samples (rutin and Rut-L-Pro) were put into 15 mL of buffer (at nonsink condition), the suspension was stirred at 50 rpm, and the temperature was set as 37 °C. After 2, 5, 10, 15, 30, 45, 60, 90, and 120 min, about 0.5 mL of the suspension was collected and then centrifuged for 3 min. The supernatant was diluted with 0.4 mL of methanol to 0.8 mL, and the concentration was analyzed by high-performance liquid chromatography (HPLC). The remaining powder was collected and used for PXRD analysis.

An Agilent 1260 series HPLC (Agilent Technologies Co., Ltd., Santa Clara, CA) with a quaternary pump (G1311C) and a diodearray detector (G1315D) was used to analyze the concentration of rutin. A 4.6 \times 150 mm², 5 μm Agilent ZORBAX Eclipse Plus C18 column was chosen for analysis. The injection volume was set as 10 μL . The wavelength at 256 nm and the column temperature at 30 °C were needed. A gradient elution method was applied, while the mobile phase included water with 0.1% trifluoroacetic acid (A) and methanol (B). The specific method is shown in Table S1.

In Vivo Pharmacokinetic Experiments in Rats. Fourteen Sprague—Dawley rats (200–250 g) were adaptively fed for 1 week and were divided into two groups randomly. The rats were fasted for 12 h and were free for water before administration. Rutin and its cocrystal were passed through 150-mesh sieves to remove the influence of the particle size. The samples were suspended in water with 0.5% CMC-Na. Rutin and its cocrystal were administered orally at a dosage of 105 mg/kg (based on the amount of rutin). The blood sample was taken from the orbital sinus at 0.33, 0.67, 1, 1.5, 2, 4, 6, 8, and 10 h after administration. All of the blood samples were put into tubes with a heparin sodium solution. The blood samples were centrifuged, and the supernatant was collected to obtain the plasma sample. It is stored at -80 °C. After blood collection, the rats used in the experiment were euthanized with carbon dioxide.

The accurate concentration of rutin was analyzed by liquid chromatography—mass spectrometry (LC–MS). First, 20 μ L of the mixture of β -glucuronidase (500 units/mL in pH 6.8 buffer) and sulfatase (100 units/mL in pH 6.8 buffer) was added to 100 μ L of thawing plasma sample and incubated at 37 °C for 1 h. Rutin in plasma was extracted by methanol, 600 μ L of methanal was added into the plasma sample, and the mixture was mixed through a vortex mixer for 30 min. The mixture was centrifuged at 14,000 rpm for 5 min, and the supernatant was used for quantification.

A SCIEX Triple QuadTM 4500 LC–MS instrument was used to analyze the concentration of rutin in plasma. We employed multiple reaction monitoring modes (MRM), and the m/z was $609.2 \rightarrow 300$. The column temperature was set to 30 °C. A gradient elution method was applied, and the mobile phase consisted of water with 1 mmol/L ammonium formate (A) and methanol with 1 mmol/L ammonium formate (B). The specific method is shown in Table S2.

All of the pharmacokinetic experiments followed the Guide for Care and Use of Laboratory Animals, and the Animal Care and Use Committee of the Shanghai Institute of Material Medica provided support.

Evaluation of the Blood Glucose Control Effect. Streptozotocin-induced diabetic models: Before the experiment, 150 Sprague—Dawley rats (200—250 g) were adaptively fed for 1 week. Eight rats were chosen as normal control and were treated with equivalent citrate buffer. The other intraperitoneal injected streptozotocin (STZ) was freshly dissolved in citrate buffer at a dosage of 60 mg/kg. The FBG was measured on days 2 and 7 after injection. Rats with blood glucose concentrations of more than 11.1 mmol/L but less than 30 mmol/L were used for the study.

Experimental protocol: During this study, 64 rats were selected; 56 were STZ-induced diabetic rats, and 8 were normal. The rats were allotted into eight groups, which were the normal control groups, diabetic control group, rutin, and Rut-L-Pro with low, moderate, and high doses. The low, moderate, and high doses were 50, 100, and 300 mg/kg, respectively (based on the amount of rutin). The diabetic control group was treated with an equivalent vehicle, and the normal control group received 100 mg/kg Rut-L-Pro (in terms of rutin). All of the rats were administered orally by intragastric administration, with the sample suspended in soybean oil for 40 days.

FBG and glucose tolerance test: After 40 days of administration, rats were fasted for 4 h and were free for water. Then, the FBG levels were measured 3–5 times. After detection of FBG, the rats were treated with rutin and Rut-L-Pro as mentioned above, and then the rats were orally administered with 2 g/kg glucose solution. The blood glucose levels were detected after 0.5 and 2 h. The area under the blood glucose response curve was calculated.

All of the experiments followed the Guide for Care and Use of Laboratory Animals, and the Animal Care and Use Committee of the Shanghai Institute of Material Medica provided support.

Evaluation of Cardioprotective Property. Experimental protocol: 32 Sprague—Dawley rats (200—250 g) were adaptively fed for 1 week and were divided into 4 groups randomly. The rats except the normal control group were injected subcutaneously with 3 mg/kg isoprenaline freshly dissolved in saline at day 0, followed by 1 mg/kg for 14 days. The normal control group received an equivalent vehicle. The Rut group was treated with 100 mg/kg rutin at the beginning of the injection, and the Rut-L-Pro group received Rut-L-Pro at a dosage of 127.70 mg/kg (equivalent to 100 mg/kg rutin) at the same time.

Measurement of the cardiac weight index (CWI): After blood collection, the hearts were excised rapidly and flushed with saline. The hearts were weighed subsequently. The CWI was calculated as the heart mass divided by body weight.

Measurement of the myocardial enzyme and antioxidant enzyme levels in serum: The blood was collected from the abdominal aorta. The serum samples were collected and stored at $-80\,^{\circ}$ C. The levels of SOD, CK, CK-MB, and LDH were determined according to the instructions for the biochemical assay kit.

Cardiac histology examination: After 14 days of administration, the hearts were excised and fixed in a 4% polyformaldehyde solution, embedded in paraffin, and sectioned for Masson staining.

All of the experiments followed the Guide for Care and Use of Laboratory Animals, and the Animal Care and Use Committee of the Shanghai Institute of Material Medica provided support.

RESULTS AND DISCUSSION

Cocrystal Screen and Characterization. The phenolic hydroxyl groups of rutin can be regarded as hydrogen bond donors and acceptors and seemly form hydrogen bonds with the compounds with carboxyl groups, amide groups, and pyridine. Accordingly, we chose more than 40 compounds containing these groups as coformers, and two cocrystals of rutin with L-proline and D-proline were finally obtained.

The disappearance of the diffraction peaks belonging to the API and coformers and the appearance of new diffraction peaks implied the generation of a new solid form. The PXRD pattern of cocrystals compared with rutin is shown in Figure 1.

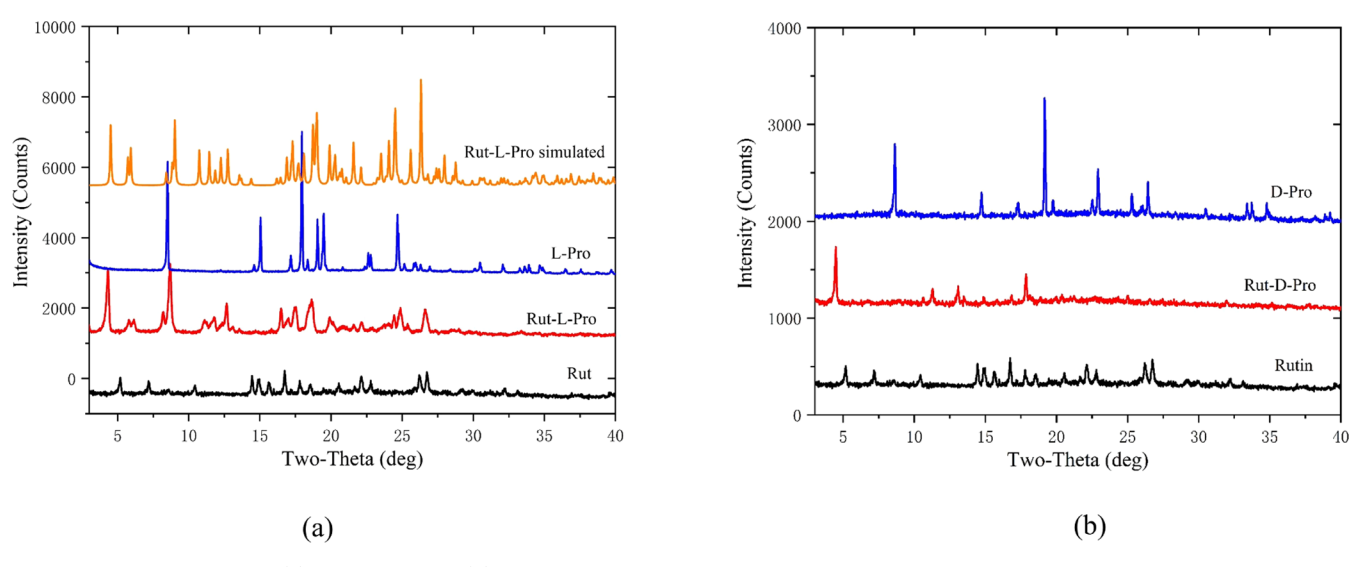


Figure 1. PXRD patterns of (a) Rut-D-Pro and (b) Rut-D-Pro.

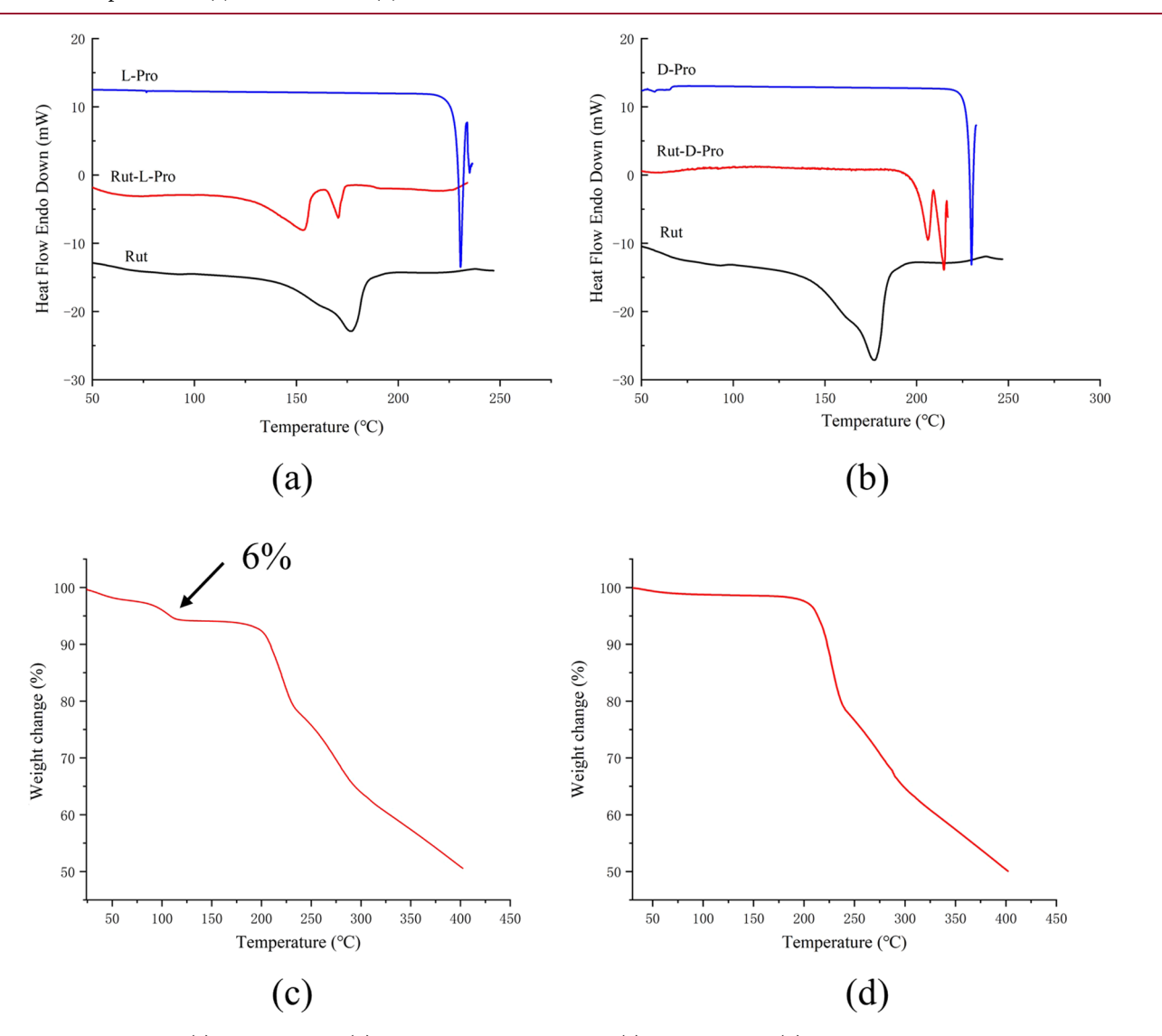
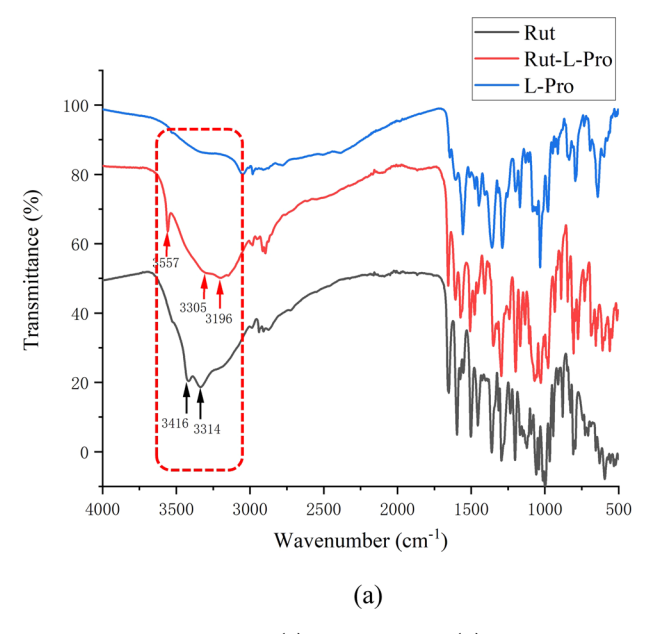


Figure 2. DSC profiles of (a) Rut-L-Pro and (b) Rut-D-Pro. TGA profiles of (c) Rut-L-Pro and (d) Rut-D-Pro.

As shown in Figure 1, there were new diffraction peaks at 2θ = 4.3, 5.8, 6.1, 8.2, 8.7, 11.1, 11.8, 12.7, 16.5, 17.5, 18.6, 19.9,

22.1, 24.4, 24.9, and 26.6°, while the characteristic peaks of rutin disappeared when formed a cocrystal with L-proline. Rut-



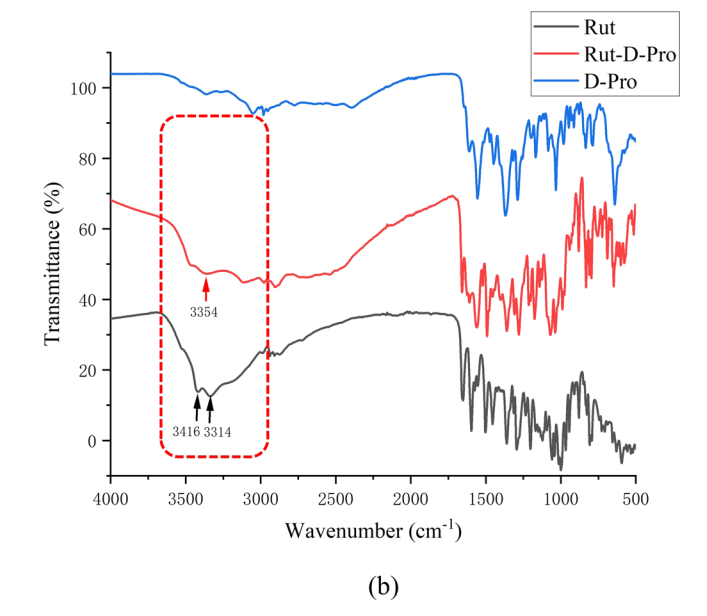
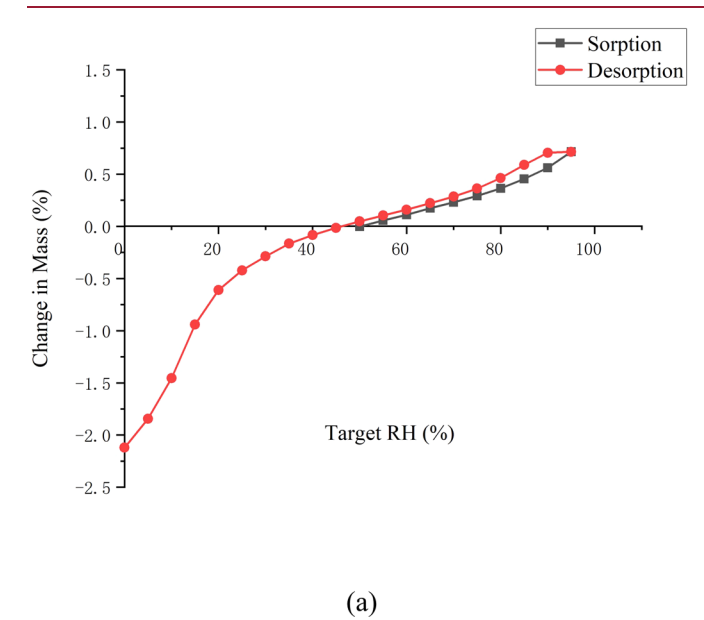


Figure 3. FT-IR spectra of (a) Rut-L-Pro and (b) Rut-D-Pro.



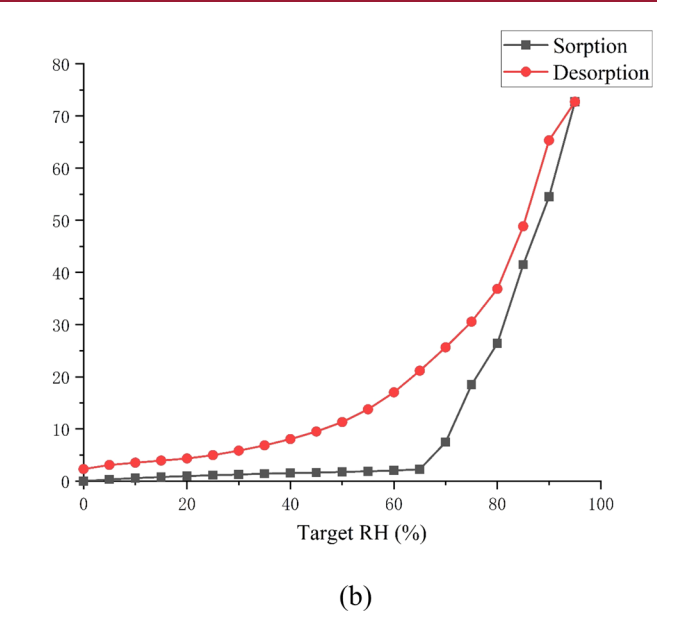


Figure 4. DVS profiles of (a) Rut-L-Pro and (b) Rut-D-Pro.

D-Pro has new diffraction peaks at 2θ = 4.5, 10.7, 11.3, 13.1, 13.5, 14.9, 16.8, 17.9, 20.4,25.0, and 28.3°.

The thermal analysis such as DSC can help confirm if there were new solid forms and whether the products had sufficient phase purity. TGA can determine if there were solvents remaining on the surface or in the lattice. The results are displayed in Figure 2. Taking Rut-L-Pro as an example, an obvious weight loss of about 6% in the range of 40–150 °C can be seen, which indicated that there was residual water (calculated at 6.9% for $3H_2O$). The analysis of the single-crystal structure proved that there were three water molecules in the lattice. Moreover, the DSC pattern of Rut-D-Pro had two endothermic peaks, which corresponded to the melt and decomposition of Rut-D-Pro, respectively. There was no obvious weight change, and the moisture content of Rut-D-Pro also proved that this form was not a hydrate. The DSC

pattern of Rut-D-Pro implied that the production was a new solid form and had sufficient phase purity.

The formation of hydrogen bonds between API and coformers leads to the FT-IR spectrum of API getting changed. The stretching vibration band of O-H in rutin was at 3416 and 3314 cm⁻¹. When the API cocrystallized with the coformers, the band had a significant shift. For instance, when forming a cocrystal with L-proline, the O-H stretching vibration bands at 3416 and 3314 cm⁻¹ shifted to 3305 and 3196 cm⁻¹, respectively, because the intermolecular hydrogen bond became a broad brand. A sharp brand at 3557 cm⁻¹ appeared, which may correspond to the free hydroxyl group. Besides, the band of O-H stretching vibration changed obviously in Rut-D-Pro compared with rutin. The band shifted to 3354 cm⁻¹ and changed to a broad brand. The FT-IR spectra can be seen in Figure 3.

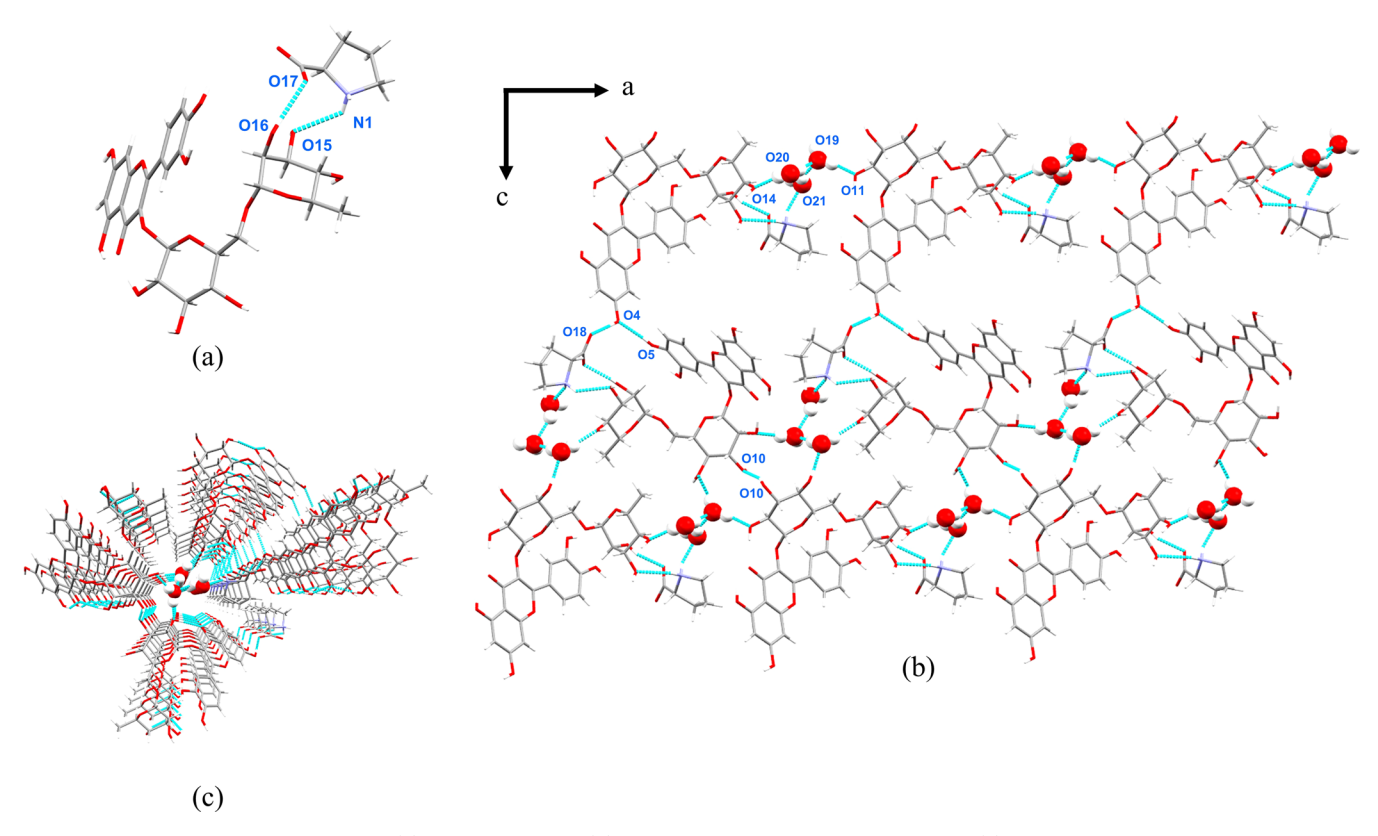


Figure 5. Crystal structure of Rut-L-Pro: (a) asymmetric unit, (b) a 2D layer parallel to the ac plane, and (c) the interaction between the two planes and the H_2O molecules extend longitudinally along the b-axis.

The moisture sorption and desorption curves of rutin cocrystals are shown in Figure 4. A slight mass change can be observed in the sorption process of Rut-L-Pro, while a significant mass change occurred for Rut-D-Pro, and the mass changes were about 0.7 and 70%, respectively. The PXRD pattern of the samples after DVS detection (Figure S2) indicated that no phase transformation occurred during the detection of Rut-L-Pro. The PXRD patterns of the samples at RH 0% and RH 95% were also detected. As shown in Figure S2a, Rut-L-Pro remains stable under the conditions with low and high humidity. The cocrystal of rutin with D-proline converted to the raw material, which proved that Rut-D-Pro had poor stability and Rut-L-Pro was stable.

Single-Crystal Structure. The single crystal of Rut-L-Pro was obtained by slow evaporation in a mixed solvent composed of 50% methanol and 50% ethyl acetate. It belonged to the monoclinic P21 space group. Each asymmetric contained one rutin molecule, one L-proline molecule, and three H₂O molecules. The crystallographic data are displayed in Table S3, and hydrogen bond parameters are listed in Table S4. The API and the coformer were connected with each other via N1-H1B···O15 ($d_{(\text{D···A})}$ = 2.851 Å, 121.1°) and O16-H16··· O17 ($d_{(\text{D···A})}$ = 2.715 Å, 153.8°), resulting in an R2 2(10) graph net, and the structure is shown in Figure 5a. The asymmetric units were connected with each other through O20-H20B···O14 ($d_{(D··A)} = 2.655 \text{ Å}, 166.7^{\circ}$), O20-H20A··· O19 ($d_{(D\cdots A)} = 2.604$ Å, 175.6°), and O19–H19A···O11 ($d_{(D\cdots A)} = 2.652$ Å, 159.7°) and extended into a onedimensional (1D) chain along the a-axis. The intermolecular interaction is shown in Figure 5b. The 1D chain extended into a two-dimensional (2D) plane through the hydrogen bond between the phenolic hydroxyl on the benzene and the

phenolic hydroxyl on the benzopyran of another API molecule (O5–H5···O4 ($d_{(\mathrm{D···A})}=2.748$ Å, 171.8°)) and the hydrogen bond between the hydroxyl on the glucose (O10–H10···O10 ($d_{(\mathrm{D···A})}=2.945$ Å, 159.1°)), which is shown in Figure 5b. The 2D layer expanded into a three-dimensional (3D) structure via the combination of the esoporous O15–H15···O16 ($d_{(\mathrm{D···A})}=2.887$ Å, 127.5°) and the esoporous O14–H14···O16 ($d_{(\mathrm{D···A})}=2.785$ Å, 155.5°). The coformer hung on the outside and extended along the *b*-axis through N1–H1B···O17 ($d_{(\mathrm{D···A})}=3.062$ Å, 128.0°), as shown in Figure 5c. The H₂O molecules were connected with the coformer through N1–H1A···O21 ($d_{(\mathrm{D···A})}=2.814$ Å, 148.3°) and connected with other H₂O molecules via the interactions of O20–H20A···O19 ($d_{(\mathrm{D···A})}=2.604$ Å, 175.6°) and O21–H21B···O19 ($d_{(\mathrm{D···A})}=2.805$ Å, 146.3°).

Solubility and Dissolution Research. Regarding the poor stability of Rut-D-Pro, we tested the solubility and dissolution behavior of rutin and Rut-L-Pro in pH 2.0, 4.5, and 6.8 buffers.

First, the powder dissolution experiments were carried out. The results of powder dissolution experiments are illustrated in Figure 6. The dissolution profiles suggested that the dissolution rate of Rut-L-Pro was significantly superior to that of rutin. In different buffers, with the collapse of the cocrystal structure, the cocrystal dissolved rapidly and reached a high supersaturation level (about 2 mg/mL), which was 20-fold that of rutin (less than 100 μ g/mL). With the recrystallization of API, the supersaturation level cannot be maintained. Within 1 h, the cocrystal exhibited 3-fold dissolution advantages, while the solubility of the cocrystal was approximately 300 μ g/mL and that of rutin was approximately 100 μ g/mL. After 2 h, there was only 2-fold

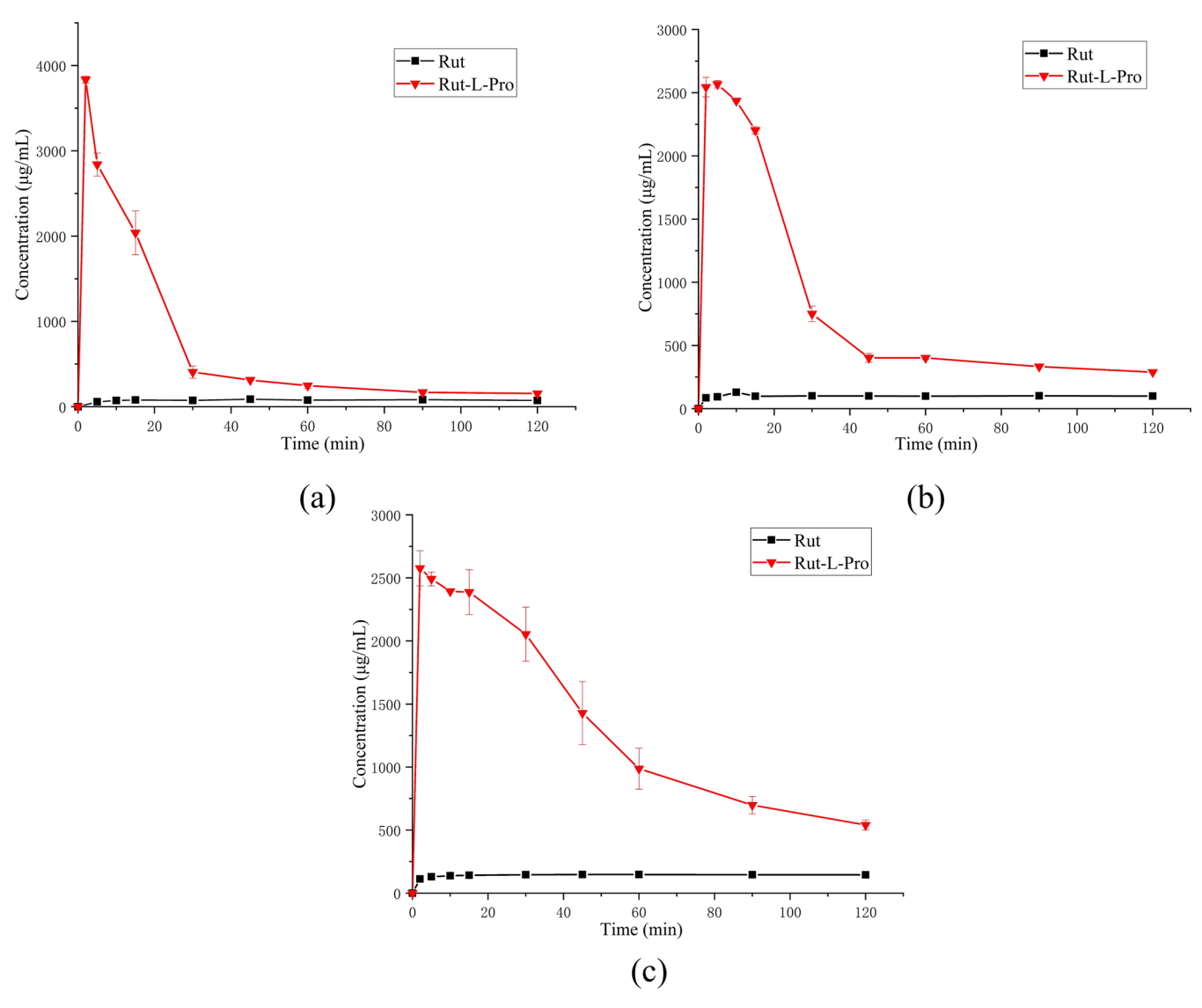


Figure 6. Powder dissolution of rutin and Rut-L-Pro in (a) pH 2.0, (b) pH 4.5, and (c) pH 6.8.

supersaturation; the cocrystal was about 200 μ g/mL and the rutin was about 100 μ g/mL. The precipitate was collected and characterized by PXRD. The PXRD pattern indicated that the cocrystal precipitated in the form of rutin, and the PXRD pattern can be seen in Figure S3.

Accordingly, the cocrystal of rutin with L-proline enhanced the solubility and dissolution rate of rutin sharply and can maintain certain dissolution advantages for a period of time. According to the correlation between the improved dissolution rate in vitro and the pharmacokinetic behavior in vivo, the pharmacokinetic properties of the cocrystal can be further evaluated.

Pharmacokinetic Research. Rut-L-Pro was chosen to conduct the pharmacokinetic research according to the results of dissolution and stability studies. The rats were treated with 105 mg/kg rutin. The profile of rutin blood concentration versus time is demonstrated in Figure 7, and the PK parameters are illustrated in Table 1. As shown in Figure 7, it was obvious that the oral bioavailability of rutin was notably improved by cocrystallization. According to the profile, the $C_{\rm max}$ of Rut-L-Pro was 3.8-fold that of rutin, and AUC $_{\rm 0-10h}$ was 5.6-fold. As mentioned above, the cocrystal exhibited much higher bioavailability, with better application prospects.

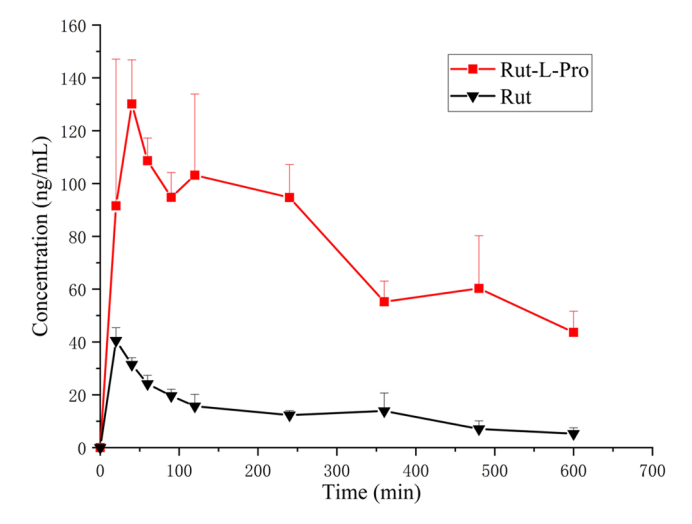


Figure 7. Rutin concentration in plasma versus time curves of rutin and Rut-L-Pro.

Pharmacodynamic Evaluation. Blood Glucose Control Effect. Diabetes is a severe metabolic disorder disease with an

Table 1. Pharmacokinetic Parameters of Rutin and Rut-L-Pro^a

	Rut	Rut-L-Pro
$C_{\text{max}} (\text{ng/mL})$	39.48 ± 4.40	$152.34 \pm 33.62*$
$T_{\rm max}$ (h)	0.33	0.81 ± 0.54
AUC (ng·min/mL)	8116.58 ± 1474.77	45573.58 ± 3303.91*

[&]quot;Values with "*" differ significantly from the group treated with rutin (P < 0.05).

increased risk of pathological change in various organs.³⁸ Increasingly evidence proved that rutin has a beneficial effect on blood glucose control and diabetic complications.³⁹ Therefore, the fast blood glucose control effects of rutin and its cocrystals were evaluated.

The FBG is a commonly used index for diabetes mellitus and reflects the secretion of insulin by the pancreatic islets. The antihyperglycemic effect of rutin and its cocrystal at different doses is illustrated in Table S5 and Figure 8. As

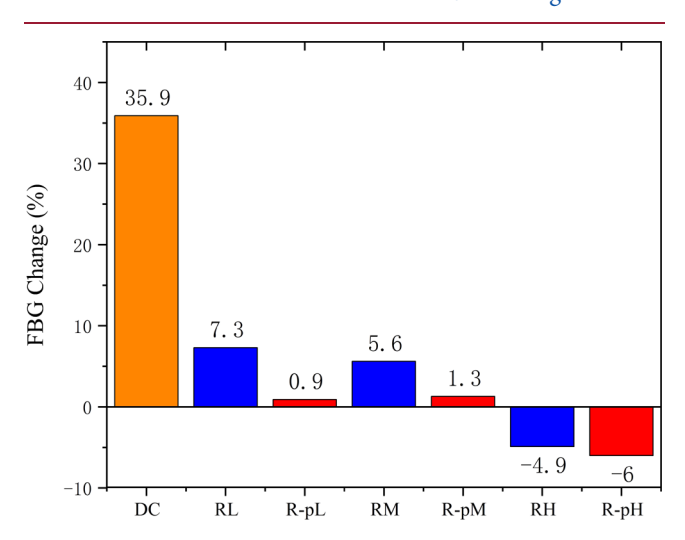


Figure 8. Effect of Ru and its cocrystal on FBG.

shown in Table S5 and Figure 8, a significant increase in FBG (35.9%) was observed in the diabetic control group, and the FBG of rats treated with rutin and its cocrystals remained stable. The results showed that the cocrystal has a more obvious effect on blood glucose control. Rats received 64 mg/kg Rut-L-Pro (equivalent to 50 mg/kg rutin) and showed a great blood glucose control effect (only increased by 0.9%), while rutin at the same dose rose 7.3%, indicating that the rutin cocrystal had a better effect on reducing FBG. The result was consistent with the increased bioavailability of Rut-L-Pro. Besides, the samples exhibited a better blood glucose control effect with the increase of dosage for both rutin and Rut-L-Pro. The rats treated with 300 mg/kg rutin and Rut-L-Pro exhibited the most significant blood glucose control effect, decreased by 4.9 and 6.0%, respectively.

As shown in Table S6 and Figure 9, administration with rutin and its cocrystal before glucose loading can inhibit the sharp rise of the blood glucose level and manifest as a reduction of glucose tolerance. The results showed that rats that received rutin and Rut-L-Pro could decrease the $GAUC_{0-2h}$ obviously, and the effect of cocrystal was much better than rutin at the same dose. Even Rut-L-Pro with a low dose showed a much better inhibitory effect on postprandial blood glucose elevation than rutin with a high dose, with

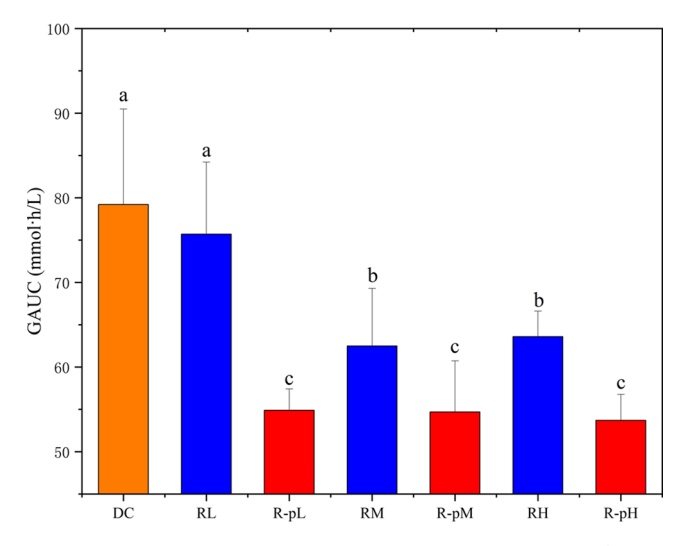


Figure 9. Effect of rutin and its cocrystal on glucose tolerance (values not sharing a common superscript (a, b, c) differ significantly from each other (P < 0.05)).

GAUC_{0-2h} values of 54.9 and 63.6 mmol·h/L, respectively. There is a significant difference (p < 0.05) between the cocrystal group and the equivalent dose of the rutin group.

Cardioprotective Property. Myocardial fibrosis is an important pathological change caused by persistent hypertension, ischemic injury, and myocardial diseases, is manifested as dysregulated collagen conversion, and results in diffuse collagen deposition in the interstitial and perivascular. The disorder of cytokines, growth factors, and reactive oxygen species are responsible for the change in the collagen matrix. A great number of studies proved that treatment with rutin can inhibit myocardial morphological changes for various reasons. Therefore, the cardioprotective properties of rutin and its cocrystals were evaluated.

To evaluate the protective effect of rutin and its cocrystal on myocardial injury, Masson-stained sections were utilized to evaluate the distribution of collagen fibers in rats' myocardial tissue, and the results are illustrated in Figure 10. According to the histopathological observation, compared with normal rats, the rats treated with ISO exhibited more fiber deposition in the myocardial interstitial. The rats treated with rutin alleviated the fiber deposition, and those administered with Rut-L-Pro exhibited a more obvious effect on decreasing fiber deposition.

ISO induction can lead to myocardial hypertrophy. As shown in Figure S4, CWI increased sharply for ISO-induced rats (5.74 mg/g) compared to the normal rats (3.54 mg/g). Treatment with rutin alleviated the symptoms (declined to 5.46 mg/g) but the effect was not significant, while the Rut-L-Pro group decreased sharply compared with the ISO group (declined to 5.09 mg/g). The myocardial enzymes were widely used for the diagnosis of heart disease clinically. In this experiment, ISO-induced myocardial injury results in a significant increase of CK, CK-MB, and LDH levels (p < 0.05), as shown in Figure 11. Rats treated with rutin decreased the levels of CK and CK-MB but had no effect on LDH, while treatment with Rut-L-Pro significantly inhibited the elevation of CK, CK-MB, and LDH. As mentioned above, Rut-L-Pro exhibited a more obvious protective effect on myocardial injury compared with the raw material of rutin.

A great number of studies have proved that rutin can play a myocardial protective effect by improving the antioxidant

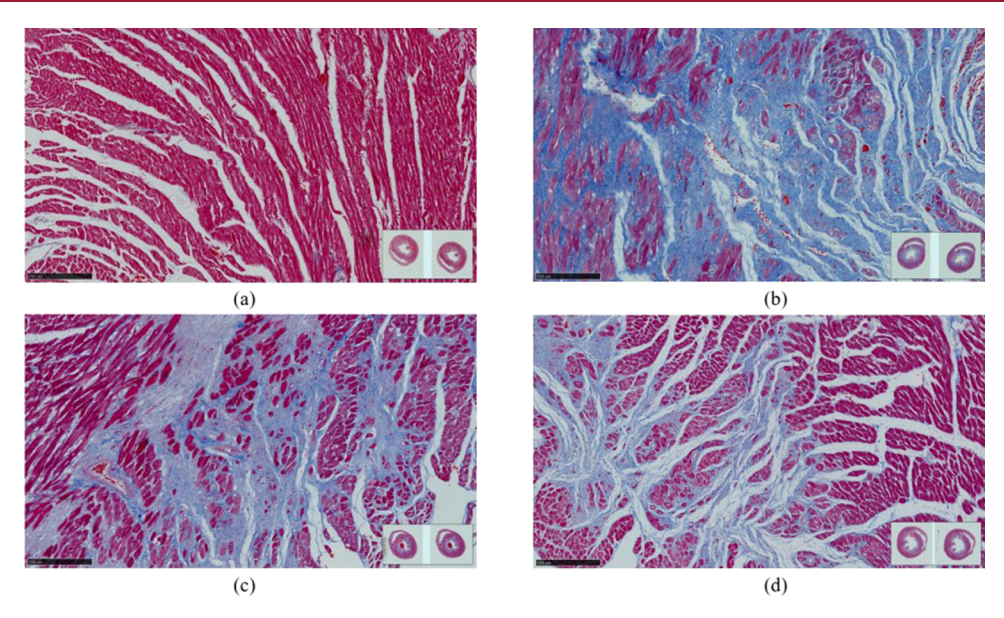


Figure 10. Effect of rutin and its cocrystal on fiber deposition in rats' myocardial tissue: (a) normal control, (b) ISO-induced myocardial fibrosis, (c) treated with rutin, and (d) treated with Rut-L-Pro.

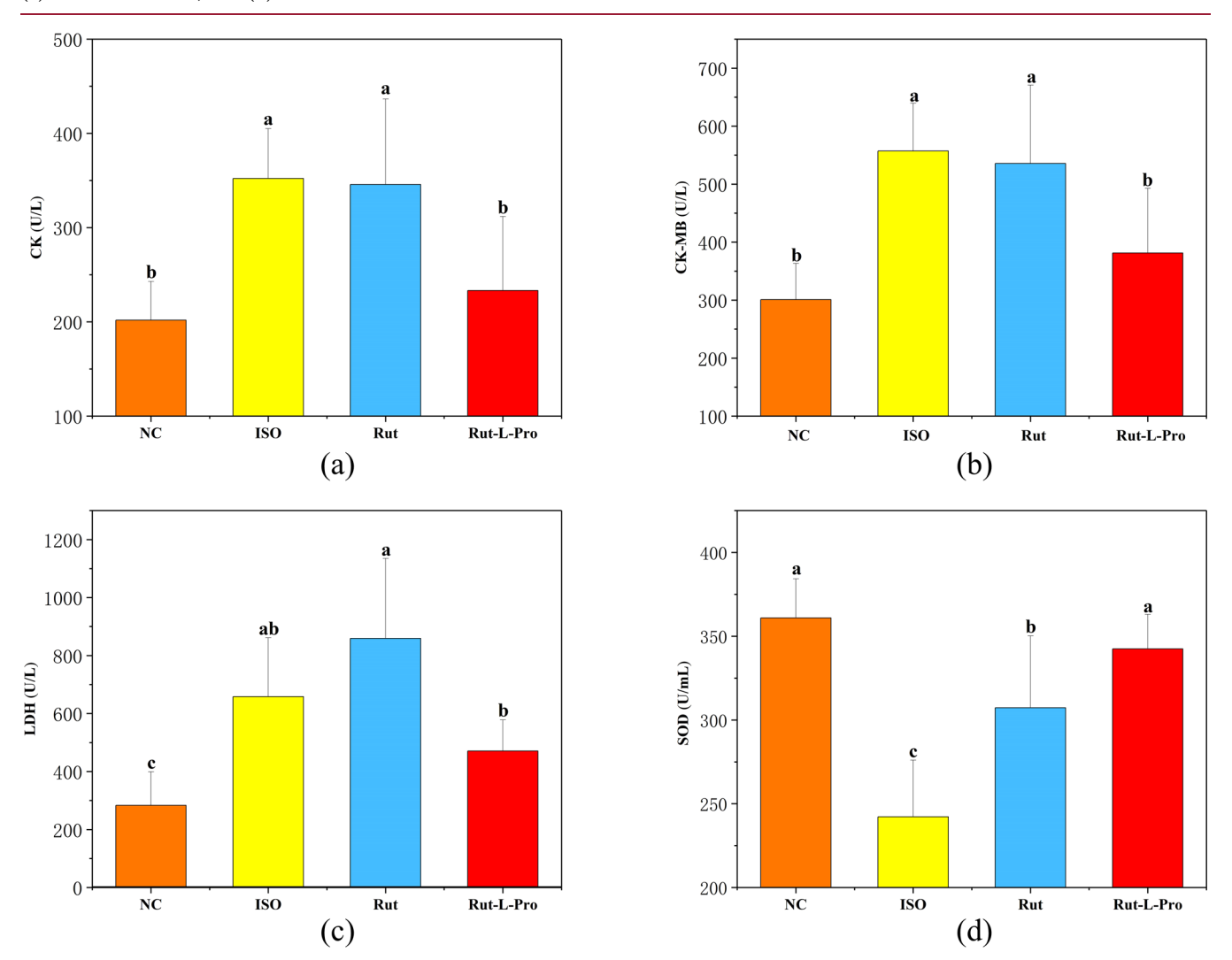


Figure 11. Effect of rutin and its cocrystal on ISO-induced myocardial fibrosis: (a) CK, (b) CK-MB, (c) LDH, and (d) SOD in serum (values not sharing a common superscript (a, b, c) differ significantly from each other (P < 0.05)).

status. Therefore, we evaluated the antioxidant enzyme (SOD) in the serum. As shown in Figure 11, the results indicated that ISO induction led to a significant decline in the activity of SOD compared with the normal rats, which were 242.23 and 360.90 U/mL, respectively, and treatment with rutin and Rut-L-Pro can both prevent the alterations in antioxidant enzymes. Rut-L-Pro exhibited a more obvious effect, which was 342.49 U/mL and was similar to the normal rats. The results of the biochemical marker test are illustrated in Figure 11 and Table S7.

CONCLUSIONS

In this study, two cocrystals of rutin with L-proline and Dproline were successfully prepared. The cocrystals were characterized carefully by PXRD, DSC, TGA, IR, and DVS, and the crystal structure of Rut-L-Pro was analyzed by SCXRD. The results indicated that Rut-L-Pro presented improved physicochemical properties. The solubility and dissolution rate of rutin and Rut-L-Pro were further analyzed in different buffers. It proved that Rut-L-Pro had a significantly improved dissolution performance in vitro, which was about 20-fold that of parent rutin in pH 2.0, 4.5, and 6.8 buffers. The result of the pharmacokinetic experiment in vivo was consistent with the improvement of solubility in water. AUC_{0-10h} was 5.6-fold, while C_{max} was 3.8-fold that of rutin. The results of the evaluation of pharmacodynamic efficacy proved that Rut-L-Pro showed a more obvious blood glucose control effect and cardioprotective activity, which may be attributed to the improvement of absorption of rutin. In conclusion, Rut-L-Pro can be a better solid form with potential application value.

ASSOCIATED CONTENT

Solution Supporting Information

The Supporting Information is available free of charge at https://pubs.acs.org/doi/10.1021/acs.cgd.4c00430.

¹H NMR of rutin and D-proline (Figure S1); HPLC mobile phase (Table S1); LC-MS mobile phase (Table S2); PXRD pattern of rutin cocrystals after DVS detection: (a) Rut-L-Pro and (b) Rut-D-Pro (Figure S2); crystallographic data of Rut-L-Pro (Table S3); hydrogen bond parameters (Table S4); PXRD pattern of precipitation obtained from dissolution (Figure S3); effect of rutin and its cocrystal on FBG (Table S5); effect of rutin and its cocrystal on glucose tolerance (Table S6); effect of rutin and its cocrystal on ISO-induced myocardial fibrosis (Table S7); and effect of rutin and its cocrystal on the cardiac weight index (Figure S4) (PDF)

Accession Codes

CCDC 2323197 contains the supplementary crystallographic data for this paper. These data can be obtained free of charge via www.ccdc.cam.ac.uk/data_request/cif, or by emailing data_request@ccdc.cam.ac.uk, or by contacting The Cambridge Crystallographic Data Centre, 12 Union Road, Cambridge CB2 1EZ, UK; fax: +44 1223 336033.

AUTHOR INFORMATION

Corresponding Authors

Jian-Rong Wang – Pharmaceutical Analytical & Solid-State Chemistry Research Center, Shanghai Institute of Materia Medica, Chinese Academy of Sciences, Shanghai 201203, China; orcid.org/0000-0002-0853-7537; Email: jrwang@simm.ac.cn

Xuefeng Mei — Pharmaceutical Analytical & Solid-State Chemistry Research Center, Shanghai Institute of Materia Medica, Chinese Academy of Sciences, Shanghai 201203, China; University of Chinese Academy of Sciences, Beijing 100049, China; School of Chinese Materia Medica, Nanjing University of Chinese Medicine, Nanjing 210023, China; orcid.org/0000-0002-8945-5794; Email: xuefengmei@simm.ac.cn

Authors

Bingrui Zhang — Pharmaceutical Analytical & Solid-State Chemistry Research Center, Shanghai Institute of Materia Medica, Chinese Academy of Sciences, Shanghai 201203, China; University of Chinese Academy of Sciences, Beijing 100049, China

Lei Tang – Pharmaceutical Analytical & Solid-State Chemistry Research Center, Shanghai Institute of Materia Medica, Chinese Academy of Sciences, Shanghai 201203, China; University of Chinese Academy of Sciences, Beijing 100049, China

Fanyu Tian — School of Chinese Materia Medica, Nanjing University of Chinese Medicine, Nanjing 210023, China Qiaoce Ding — Pharmaceutical Analytical & Solid-State Chemistry Research Center, Shanghai Institute of Materia Medica, Chinese Academy of Sciences, Shanghai 201203, China

Ziyi Hu — Pharmaceutical Analytical & Solid-State Chemistry Research Center, Shanghai Institute of Materia Medica, Chinese Academy of Sciences, Shanghai 201203, China; University of Chinese Academy of Sciences, Beijing 100049, China

Complete contact information is available at: https://pubs.acs.org/10.1021/acs.cgd.4c00430

Funding

This research was funded by the Natural Science Foundation of Shanghai (Grant No. 43322ZR1473900).

Notes

The authors declare no competing financial interest.

ACKNOWLEDGMENTS

The authors thank the Shanghai Natural Science Foundation (Grant No. 43322ZR1473900) for funding.

REFERENCES

- (1) Gullón, B.; Lú-Chau, T. A.; Moreira, M. T.; Lema, J. M.; Eibes, G. Rutin: A review on extraction, identification and purification methods, biological activities and approaches to enhance its bioavailability. *Trends Food Sci. Technol.* **2017**, *67*, 220–235.
- (2) Boyle, S. P.; Dobson, V. L.; Duthie, S. J.; Hinselwood, D. C.; Kyle, J. A.; Collins, A. R. Bioavailability and efficiency of rutin as an antioxidant: a human supplementation study. *Eur. J. Clin. Nutr.* **2000**, *54* (10), 774–782.
- (3) Habtemariam, S. Antioxidant and rutin content analysis of leaves of the common buckwheat (fagopyrum esculentum moench) grown in the United Kingdom: A case study. *Antioxidants* **2019**, 8 (6), 160–160
- (4) Kessler, M.; Ubeaud, G.; Jung, L. Anti- and pro-oxidant activity of rutin and quercetin derivatives. *J. Pharm. Pharmacol.* **2010**, 55 (1), 131–142.
- (5) Guardia, T.; Rotelli, A. E.; Juarez, A. O.; Pelzer, L. E. Anti-inflammatory properties of plant flavonoids. Effects of rutin, quercetin

and hesperidin on adjuvant arthritis in rat. Il Farmaco 2001, 56 (9), 683-687.

- (6) Lee, Y. J.; Jeune, K. H. The Effect of Rutin on Antioxidant and Anti-inflammation in Streptozotocin-induced Diabetic Rats. *Appl. Microsc.* **2013**, 43 (2), 54–64.
- (7) Chen, T.-H.; Tsai, M.-J.; Chang, C.-S.; Xu, L.; Fu, Y.-S.; Weng, C.-F. The exploration of phytocompounds theoretically combats SARS-CoV-2 pandemic against virus entry, viral replication and immune evasion. *J. Infect. Public Health* **2023**, *16* (1), 42–54.
- (8) Nouri, Z.; Fakhri, S.; Nouri, K.; Wallace, C. E.; Farzaei, M. H.; Bishayee, A. Targeting multiple signaling pathways in cancer: The rutin therapeutic approach. *Cancers* **2020**, *12* (8), 2276–2309.
- (9) ben Sghaier, M.; Pagano, A.; Mousslim, M.; Ammari, Y.; Kovacic, H.; Luis, J. Rutin inhibits proliferation, attenuates superoxide production and decreases adhesion and migration of human cancerous cells. *Biomed. Pharmacother.* **2016**, *84*, 1972–1978.
- (10) Budzynska, B.; Faggio, C.; Kruk-Slomka, M.; Samec, D.; Nabavi, S. F.; Sureda, A.; Devi, K. P.; Nabavi, S. M. Rutin as neuroprotective agent: from bench to bedside. *Curr. Med. Chem.* **2019**, *26* (27), 5152–5164.
- (11) De Araújo, F. M.; Frota, A. F.; de Jesus, L. B.; Cuenca-Bermejo, L.; Ferreira, K. M. S.; Santos, C. C.; Soares, E. N.; Souza, J. T.; Sanches, F. S.; Costa, A. C. S.; Farias, A. A.; de Fatima Dias Costa, M.; Munoz, P.; Menezes-Filho, J. A.; Segura-Aguilar, J.; Costa, S. L.; Herrero, M. T.; Silva, V. D. A. Protective Effects of Flavonoid Rutin Against Aminochrome Neurotoxicity. *Neurotoxic. Res.* **2023**, *41* (3), 224–241.
- (12) Rana, A. K.; Kumar, R.; Shukla, D. N.; Singh, D. Lithium coadministration with rutin improves post-stroke neurological outcomes via suppressing Gsk-3 β activity in a rat model. *Free Radical Biol. Med.* **2023**, 207, 107–119.
- (13) Wang, Y.-D.; Zhang, Y.; Sun, B.; Leng, X.-W.; Li, Y.-J.; Ren, L.-Q. Cardioprotective effects of rutin in rats exposed to pirarubicin toxicity. *J. Asian Nat. Prod. Res.* **2018**, *20* (4), 361–373.
- (14) Habtemariam, S.; Lentini, G. The therapeutic potential of rutin for diabetes: an update. *Mini-Rev. Med. Chem.* **2015**, *15* (7), 524–528.
- (15) Fernandes, A. A. H.; Novelli, E. L. B.; Okoshi, K.; Okoshi, M. P.; Muzio, B. P. D.; Guimarães, J. F. C.; Junior, A. F. Influence of rutin treatment on biochemical alterations in experimental diabetes. *Biomed. Pharmacother.* **2010**, *64* (3), 214–219.
- (16) Yang, J.; Guo, J.; Yuan, J. In vitro antioxidant properties of rutin. LWT Food Sci. Technol. 2008, 41 (6), 1060-1066.
- (17) Siti, H. N.; Jalil, J.; Asmadi, A. Y.; Kamisah, Y. Roles of rutin in cardiac remodeling. *J. Funct. Foods* **2020**, *64*, 103606–103617.
- (18) Xianchu, L.; Lan, Z.; Ming, L.; Yanzhi, M. Protective effects of rutin on lipopolysaccharide-induced heart injury in mice. *J. Toxicol. Sci.* **2018**, 43 (5), 329–337.
- (19) Saklani, R.; Gupta, S. K.; Mohanty, I. R.; Kumar, B.; Srivastava, S.; Mathur, R. Cardioprotective effects of rutin via alteration in TNF- α , CRP, and BNP levels coupled with antioxidant effect in STZ-induced diabetic rats. *Mol. Cell. Biochem.* **2016**, 420 (1–2), 65–72.
- (20) Li, Y. Q.; Zhou, F. C.; Gao, F.; Bian, J. S.; Shan, F. Comparative Evaluation of Quercetin, Isoquercetin and Rutin as Inhibitors of α -Glucosidase. *J. Agric. Food Chem.* **2009**, *57* (24), 11463–11468.
- (21) Esmaeili, M. A.; Zohari, F.; Sadeghi, H. Antioxidant and Protective Effects of Major Flavonoids from Teucrium polium on β -Cell Destruction in a Model of Streptozotocin-Induced Diabetes. *Planta Med.* **2009**, 75 (13), 1418–1420.
- (22) Kappel, V. D.; Cazarolli, L. H.; Pereira, D. F.; Postal, B. G.; Zamoner, A.; Reginatto, F. H.; Silva, F. R. M. B. Involvement of GLUT-4 in the stimulatory effect of rutin on glucose uptake in rat soleus muscle. *J. Pharm. Pharmacol.* **2013**, *65* (8), 1179–1186.
- (23) Jadhav, R.; Puchchakayala, G. Hypoglycemic and antidiabetic activity of flavonoids: boswell acid, ellagic acid, quercetin, rutin on streptozotocin-nicotinamide induced type 2 diabetic rats. *Int. J. Pharm. Pharm. Sci.* **2012**, *4* (2), 251–256.
- (24) Niture, N. T.; Ansari, A. A.; Naik, S. R. Anti-hyperglycemic activity of rutin in streptozotocin-induced diabetic rats: an effect

- mediated through cytokines, antioxidants and lipid biomarkers. *Indian J. Exp. Biol.* **2014**, *52* (7), 720–727.
- (25) Manach, C.; Morand, C.; Demigné, C.; Texier, O.; Régérat, F.; Rémésy, C. Bioavailability of rutin and quercetin in rats. *FEBS Lett.* **1997**, 409 (1), 12–16.
- (26) Wang, Q.; Huang, J.; Hu, C.; Xia, N.; Li, T.; Xia, Q. Stabilization of a non-aqueous self-double-emulsifying delivery system of rutin by fat crystals and nonionic surfactants: preparation and bioavailability study. *Food Funct.* **2017**, 8 (7), 2512–2522.
- (27) Negahdari, R.; Bohlouli, S.; Sharifi, S.; Dizaj, S. M.; Saadat, Y. R.; Khezri, K.; Jafari, S.; Ahmadian, E.; Jahandizi, N. G.; Raeesi, S. Therapeutic benefits of rutin and its nanoformulations. *Phytother. Res.* **2021**, 35 (4), 1719–1738, DOI: 10.1002/ptr.6904.
- (28) Van Khanh, N.; Thu, T. T.; Tuan, H. A. Preparation of solid dispersion of rutin by spay drying. *VUN J. Sci.: Med. Pharm. Sci.* **2019**, 35 (2), 27–36, DOI: 10.25073/2588-1132/vnumps.4191.
- (29) De Gaetano, F.; Cristiano, M. C.; Venuti, V.; Crupi, V.; Majolino, D.; Paladini, G.; Acri, G.; Testagrossa, B.; Irrera, A.; Paolino, D.; Tommasini, S.; Ventura, C. A.; Stancanelli, R. Rutin-Loaded Solid Lipid Nanoparticles: Characterization and In Vitro Evaluation. *Molecules* 2021, 26, No. 1039, DOI: 10.3390/molecules26041039.
- (30) Mauludin, R.; Müller, R. H.; Keck, C. M. Development of an oral rutin nanocrystal formulation. *Int. J. Pharm.* **2009**, *370* (1–2), 202–209.
- (31) Mauludin, R.; Müller, R. H.; Keck, C. M. Kinetic solubility and dissolution velocity of rutin nanocrystals. *Eur. J. Pharm. Sci.* **2009**, *36* (4), 502–510.
- (32) Ismail, A.; El-Biyally, E.; Sakran, W. An innovative approach for formulation of rutin tablets targeted for colon cancer treatment. *AAPS PharmSciTech* **2023**, 24 (2), 68–81.
- (33) Paczkowska, M.; Mizera, M.; Piotrowska, H.; Szymanowska-Powałowska, D.; Lewandowska, K.; Goscianska, J.; Pietrzak, R.; Bednarski, W.; Majka, Z.; Cielecka-Piontek, J. Complex of rutin with β -Cyclodextrin as potential delivery system. *Plos One* **2015**, *10* (3), No. e0120858.
- (34) Jin, G. Z.; Yamagata, Y.; Tomita, K. Structure of rutin pentamethanol. *Chem. Pharm. Bull.* **1990**, 38 (2), 297–300.
- (35) Aitipamula, S.; Banerjee, R.; Bansal, A. K.; Biradha, K.; Cheney, M. L.; Choudhury, A. R.; Desiraju, G. R.; Dikundwar, A. G.; Dubey, R.; Duggirala, N.; Ghogale, P. P.; Ghosh, S.; Goswami, P. K.; Goud, N. R.; Jetti, R. R. K. R.; Karpinski, P.; Kaushik, P.; Kumar, D.; Kumar, V.; Moulton, B.; Mukherjee, A.; Mukherjee, G.; Myerson, A. S.; Puri, V.; Ramanan, A.; Rajamannar, T.; Reddy, C. M.; Rodriguez-Hornedo, N.; Rogers, R. D.; Row, T. N. G.; Sanphui, P.; Shan, N.; Shete, G.; Singh, A.; Sun, C. C.; Swift, J. A.; Thaimattam, R.; Thakur, T. S.; Thaper, R. K.; Thomas, S. P.; Tothadi, S.; Vangala, V. R.; Variankaval, N.; Vishweshwar, P.; Weyna, D. R.; Zaworotko, M. J. Polymorphs, Salts, and Cocrystals: What's in a Name? *Cryst. Growth Des.* **2012**, *12* (5), 2147–2152, DOI: 10.1021/cg3002948.
- (36) Babu, N. J.; Nangia, A. Solubility Advantage of Amorphous Drugs and Pharmaceutical Cocrystals. *Cryst. Growth Des.* **2011**, *11* (7), 2662–2679.
- (37) Karimi-Jafari, M.; Padrela, L.; Walker, G. M.; Croker, D. M. Creating cocrystals: a review of pharmaceutical cocrystal preparation routes and applications. *Cryst. Growth Des.* **2018**, *18* (10), 6370–6387.
- (38) Lotfy, M.; Adeghate, J.; Kalasz, H.; Singh, J.; Adeghate, E. Chronic Complications of Diabetes Mellitus: A Mini Review. *Curr. Diabetes Rev.* **2016**, *13* (1), 3–10.
- (39) Semwal, R.; Joshi, S. K.; Semwal, R. B.; Semwal, D. K. Health benefits and limitations of rutin A natural flavonoid with high nutraceutical value. *Phytochem. Lett.* **2021**, *46*, 119–128.
- (40) Gyöngyösi, M.; Winkler, J.; Ramos, I.; Do, Q. T.; Firat, H.; McDonald, K.; González, A.; Thum, T.; Díez, J.; Jaisser, F.; Pizard, A.; Zannad, F. Myocardial fibrosis: biomedical research from bench to bedside. *Eur. J. Heart Failure* **2017**, *19* (2), 177–191.